Natural Convection From a Single Surface Heater in a Vertieal Rectangular Enclosure

الحمل الطبيعى من مسخن احادى سطحى فى حيز رأسى مستطيل

M.S. El-Kady and F. F. Araid
Mechanical Power Engineering Department
Mansoura University, Egypt

خلاصـــــة:

يتناول البحث دراسة نظرية وعملية لانتقال الحرارة بالحمل الطبيعى ثنائى البعد للهواء فى حيز قطاعه الرأسى مستطيل الشكل به منبع حرارى (مسخن) سطحى ذو فيض حرارى ثابت ومثبت على سطح رأسى معزول، بينما يبرد السطح المواجه عند درجة حرارة ثابتة والسطحين الأفقيين معزولين. تكون النموذج من معادلات الاستمرار وكمية الحركة الداخل فيها تقريب بوسينيسك والطاقة واستخدمت طريقة الفروق المحددة للحل العددى. أجريت الدراسة على حيز مستطيل الشكل ذو نسبة باعية A=2.5 ورقم رايلى يصل الى 10^7 ونسبة ارتفاع الحيز الى ارتفاع المسخن $2\le H/L\le 8$ ونسبة تغير ارتفاع المسخن الى ارتفاع الحيز $0.1\le S/H\le 0.9$.. أظهرت النتائج تأثيرا كبيرا لموضع وابعاد المسخن على شكل سريان الهائع وتوزيع درجات الحرارة ومعدل انتقال الحرارة من المسخن. كما حددت المدى الامثل لموضع وبعد المسخن للحصول على اقل درجة حرارة قصوى على سطح المسخن والحصول على أقصى قيمة لمعدل انتقال الحرارة المتوسط حيث $0.1\le S/H\le 0.5$ و $4\le H/L$. فى هذا المدى استنتجت العلاقات التالية:

$$\theta_{max} = 1.792\ Ra^{-0.18}, \qquad \bar{Nu} = 0.74\ Ra^{0.17}$$

ولاثبات صحة النموذج النظرى أجريت دراسة عملية على حيز مستطيل ذى A=2, H/L=3.33, S/H=0.5, W/L=1.66. قورنت النتائج العملية لتوزيع درجات الحرارة على السطح الرأسى للمسخن وكذلك لرقم نوسيلت الموضعى للمسخن مع النتائج العددية المناظرة لنفس الحالة أظهرت المقارنة توافقا جيدا بينهما.

Abstract:

Natural convection in a heated two-dimensional rectangular vertical enclosure is investigated numerically and experimentally for different single heater configurations. The partial differential equations governing the conservation of mass, momentum-under the Boussinesq assumption- and energy in the problem are solved numerically using the finite difference technique. The study is carried out for the steady laminar natural convection of air in a vertical enclosure with constant heat flux single heater at one adiabatic insulated vertical wall, an isothermally cooled opposing vertical wall and insulated horizontal walls. The range of parameters considered is Pr = 0.7, W/L=2, $Ra\le 10^7$, and A=2.5, $0.1\le S/H\le 0.9$ for the effect of heater location and S/H=0.4, H/L= 2, 4, 6 and 8 for the effect of heater size. The results show great effect of the heater location and size on the flow and temperature distribution inside the enclosure and heat transfer from it. A best range of heater location and heater size corresponding to maximum heat transfer and minimum value of surface heater maximum temperature is determined by $0.1\le S/H\le 0.5$ and $H/L\ge 4$ with correlations as follows:

$$\theta_{max} = 1.792\ Ra^{-0.18}, \qquad \bar{Nu} = 0.74\ Ra^{0.17}$$

Experimental tests were conducted for the case of A=2, H/L=3.33, S/H=0.5, W/L=1.66 and $Ra=7\times10^4$, 1.1×10^5 and 6.4×10^5. The experimental surface temperature and local Nusselt number were compared with the calculated results for the same case to show the validity of the numerical simulation.

Accepted August 12, 1998

Introduction

One of the serious requirements in the design and operation of modern electronic technologies has been an efficient thermal control of the system. For instant, the power densities in the state of-the-art electronic computers are extremely high. Consequently, unless an effective removal of the excessive heat geuerated within the devices in place, performance of these sensitive electronic devices deteriorates rapidly.

Extensive survey of the various modes of convective heat transfer and relevant configurations along with the associated heat transfer and other correlations have been presented by Jaluria [1], Incropera [2] and Papanicolaou and Jaluria [3]. There are some work in the literature dealing with mixed convection in the cooling of protruding heat sources of electronic components. In the work of Habchi and Arcbarya [4], the cooling of a single electronic module, treated as an isothermal protruding heat source mounted on the right wall of a vertical channel was studied. Kang et. al. [5] obtained experimental results for the cooling of a protruding heat generating module in a horizontal plate. Mahaney et al. [6] studied the mixed convective heat transfer from an array of discrete heat sources in a horizontal rectangular channel. A comprehensive analysis is made by Kim et. al. [7] of the flow and heat transfer characteristics of a mixed convection in a channel with rectangular blocks on channel wall. Papanicolaou and Jaluria [3] studied numerically the cooling of heat dissipating electronic components, located in a rectangular enclosure, and cooling is affected by externally through flow of air. Forced convection cooling of electronic equipment has been studied by many authors. Among them was Incropera et al. [8]. They studied experimentally the convection heat transfer from a two dimensional flush mounted heat sources. The developing flow and heat transfer between a series of parallel plates with surface mounted discrete heat generating blocks was studied numerically by Davalath and Bayazitoglu [9] and Kim and Anand [10-12], while the conjugate heat transfer from a single surface mounted block to forced air flow was studied experimentally and analytically by Nakayama and Park [13]. A comprehensive analysis is made by Kim et al. [14] of the flow and heat transfer characteristics of mixed convection in a channel with rectangular blocks attached on one channel. Natural convection cooling of electronic equipment continues to play a prominent role in the thermal management and control of such systems. Natural convection cooling techniques have distinct advantages because of their low cost, ease of maintenance and absence of electromaguetic interference and operating noise. Jaluria studied the buoyancy-induced flow due to isolated thermal sources on a vertical plate [15]. The natural convection between series of vertical plate channels with embedded line heat sources has been studied in order to meet the relatively lower operating temperature requirements of integrated circuits by Anand et al. [16], and Kim et al. [17,18]. Another important configuration involve complete and partial enclosures, such as those encountered in small electronic devices and personal computers. Not much work has been done on such enclosure flows, even there is a growing interest in these problems. Keyhani et al. [19] investigated experimentally natural convection flow and heat transfer characteristics of an array of discrete heat sources in enclosures. In [20], they showed the aspect ratio effect. Carmona and Keyhani [21] showed the cavity width effect on cooling of five flush heaters on one vertical wall of an enclosure.

In general, these studies illustrated the lack in knowledge about natural convection from discrete heat sources in rectangular enclosures. So, the present study supplements results in natural convection from two-dimensional heat source in the rectangular enclosures. The effect of size and location of a single heater on the temperature, local and average heat transfer are illustrated. The parameters investigated in this study include the Rayleigh number and the heat source location and size. An experimental test was performed to validate the numerical model.

Mathematical Formulation and Method of Solution

In order to formulate a mathematically tractable problem, a single module of two-dimensional steady laminar air flow driven by natural convection is considered inside a vertical rectangular enclosure of height H and width W, as illustrated in Fig. 1. The horizontal surfaces of the enclosure are adiabatic. Planar finite-sized heat source, with uniform heat flux output and height L, is located on a vertical adiabatic surface, while a constant temperature boundary is maintained at the other vertical surface. Assuming that the fluid properties are constant, except for density in the buoyancy term of the vertical momentum balance, the governing equations for mass, momentum-with the Bousinisq approximation-and energy in the enclosure are respectively:

$$\partial u/\partial x + \partial w/\partial y = 0 \qquad (1)$$

$$u\,\partial w/\partial x + v\,\partial w/\partial y = -1/\rho.[\partial P/\partial x] + \upsilon.[\partial^2 w/\partial x^2 + \partial^2 w/\partial y^2] \qquad (2)$$

$$u\,\partial v/\partial x + v\,\partial v/\partial y = -1/\rho.[\partial P/\partial y] - \upsilon.[\partial^2 v/\partial x^2 + \partial^2 v/\partial y^2] + g\beta(T - T_w) \qquad (3)$$

$$u\,\partial T/\partial x + v\,\partial T/\partial y = \alpha.[\partial^2 T/\partial x^2 - \partial^2 T/\partial y^2] \qquad (4)$$

and the conditions on the boundaries are $u = v = 0$, $q(0,y)$ = constant at the heat source surface (the heated section) and $\partial T(0,y)/\partial x=0$ for the unheated sections, $T(W,y)=T_w$, and $\partial T(x,0)/\partial y=\partial T(x,H)/\partial y=0$. where u, v, P, ρ, υ, and α are the velocity in the horizontal and vertical directions x and y, the pressure, the fluid density, the fluid kinematic viscosity and the thermal diffusivity respectively.

Eliminating the pressure P between equations (2) and (3), from definitions $\zeta=\partial v/\partial x-\partial w/\partial y$, $u=\partial\psi/\partial y$ and $v=-\partial\psi/\partial x$ and using the nondimensional variables: $X=x/L$, $Y=y/L$, $U=u.L/\upsilon$, $V=v.L/\upsilon$, $\omega=\zeta.L^2/\upsilon$, $\Psi=\psi/\upsilon$ and $\theta=(T-T_w)/(q.L/k)$ the dimensionless form for the governing equations (1-4) for steady natural convection in a vertical two dimensional enclosure can be written in terms of nondimensional stream function, vorticity, horizontal and vertical velocities and temperature as follows:

$$U.\partial\omega/\partial X + V.\partial\omega/\partial Y = Ra/Pr\,.\,[\partial\theta/\partial X] + [\partial^2\omega/\partial X^2 + \partial^2\omega/\partial Y^2] \qquad (5)$$

$$-\omega = \partial^2\Psi/\partial X^2 + \partial^2\Psi/\partial Y^2 \qquad (6)$$

$$U.\partial\theta/\partial X + V.\partial\theta/\partial Y = 1/Pr.[\partial^2\theta/\partial X^2 + \partial^2\theta/\partial Y^2] \qquad (7)$$

$$U=\partial\Psi/\partial Y \text{ and } V=-\partial\Psi/\partial X \qquad (8)$$

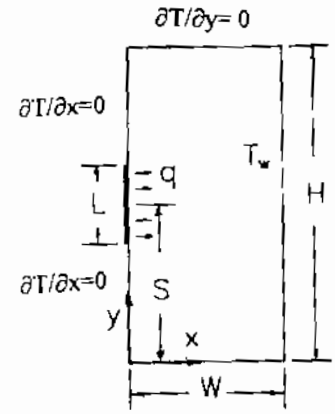

Fig. 1 Physical model, coordinate system and boundaries

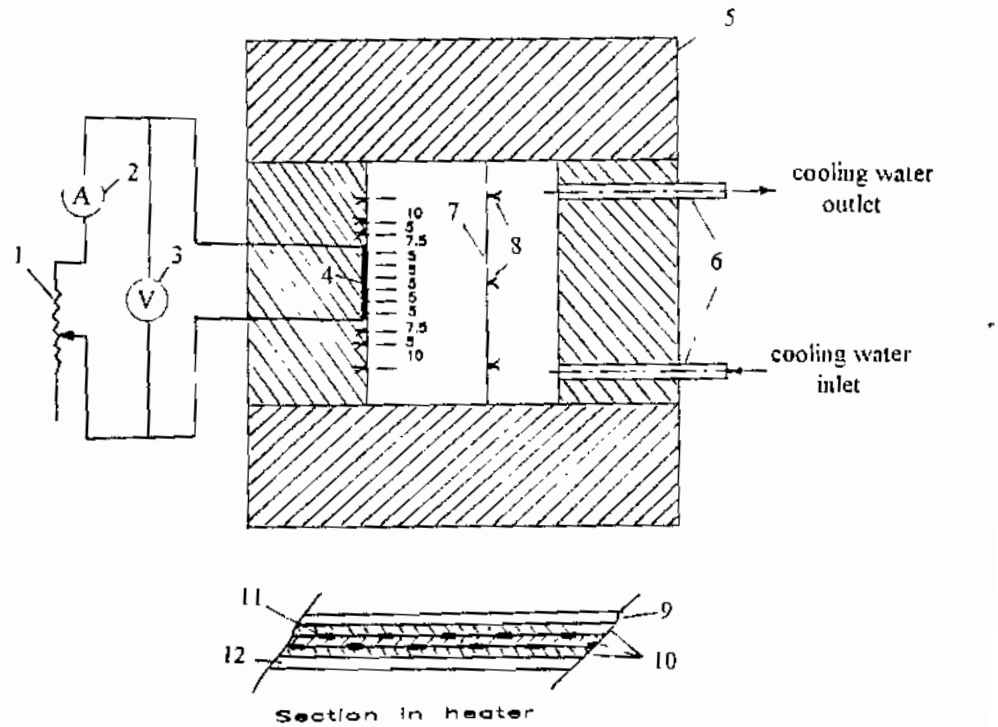

Fig. 2 Schematic diagram of the experimental apparatus

(1) auto transformer, (2) ammeter, (3) voltmeter, (4) electric heater, (5) Polyurethane insulation, (6) inlet and outlet cooling water tubes. (7) Heat exchanger, (8) copper-constantan thermocouples, (9) stainless sheet plate, (10) mica sheets (11) nickel-chromium electric heater, and (12) Thermal insulation layer.

and the dimensionless boundary conditions for the present system are

$$U = V = \Psi = 0, \text{ on all solid boundaries} \quad (9a)$$

$$\text{at } X = 0: \ \partial\theta/\partial X = -1 \text{ on heater surface,} \quad (9b)$$

$$= 0 \text{ elsewhere}$$

$$X = W/L: \ \theta = 0 \quad (9c)$$

$$Y = 0 \text{ and } H/L: \ \partial\theta/\partial Y = 0 \quad (9d)$$

where k is the thermal conductivity, Pr the Prandtle number and Ra the Rayleigh number

The dimensionless governing equations (5)-(8) and the associated boundary conditions given by equation (9) were solved by the finite difference proeedure discussed by Patanker [22]. The domain is subdivided into a number of control volumes, eaeh assoeiated with a grid point, and the governing equation is integrated over eaeh control volume resulting in a system of algebraic equations. Both the first and second order derivatives were discretized using the central difference formulas except the convection terms which were discretized by using the upwind scheme. The differenec algebraic equations are solved using the Gauss-elimination method. An iterative solution procedure was employed here to obtain the steady state solution of the problem considered. The ealculations were done on inereasingly finer grid size distributions. A 26x51 non-uniform grid with denser clustering near the walls was considered to give grid independent results. The convergence criteria used for all field variables $\xi(= \omega, \Psi, \theta)$ for every point are as follows:

$$\left|\xi^{n+1} - \xi^{n}\right|_{max} / \left|\xi^{n+1}\right|_{max} \leq 10^{-5}$$

where n is the index representing the iteration number.

Experimental Work:

In order to validate the program developed for this study, an experimental study for the air flow in a rectangular enclosure is carried out. A schematic diagram of the apparatus is shown in Fig. 2. The two dimensional reetangular enclosure used was 100 mm height and 50 mm width with an aspect ratio A=2. The enclosure was 300 mm in the spanwise direction ensuring two dimensionality of the flow and heat transfer. The right vertical wall of the enclosure was held at approximately uniform temperature by fitting a copper counter-flow heat exchanger (7) in which the city water was used as the coolant liquid. The temperature of the coolant is controlled by a constant temperature bath. Three copper-constantan thermocouples (8) were embedded in the copper wall to monitored and ensure a uniform temperature distribution. The maximum temperature variation was found to be 0.3C across the copper wall. The two horizontal surfaces were maintained nearly adiabatic by constructing them of closed-pore extruded polyurethane insulation with 50 mm thickness

The left vertical wall of the enclosure was made of the closed-pore extruded polystyrene insulation (5) of 50 mm thickness. An electric heater (4) with dimensions of 30 mm height, 2.5 mm thickness, and 300 mm long (spanwise length) was embedded in the left vertical adiabatic wall to make the heater face in the same vertical inside plane of the wall. The heater face is made of polished stainless steel sheet (9) with 0.5 mm thickness. This sheet was heated electrically by an electric heater. A nickel-chromium

wire (11) was wounded around a mica sheet (10) 0.5 mm thickness and then was sandwiched between two other mica sheets (10). The temperature distributiou along the heated and unheated parts of the vertical wall was measured by 14 copper-constantan thermocouples. Twelve thermocouples were fixed in the middle plane in the spanwise direction as shown in Fig. 2. The other 2 thermocouples were fixed in the middle height of the stainless sheet at 100 mm distance on hoth sides from the middle plane. The thermocoup'es were connected to a digital temperature recorder. The heat input to the heater was controlled by using an auto-transformer (1), au ammeter (2) and voltmeter (3). Nearly three hours were needed to reach the steady state condition. The steady state condition was recognized when tbe temperature reading did not change with time for about 15 minutes.

Results and Discussion

The effect of location and size of a single heater in a two dimensional rectangular enclosure is studied. The parameters considered in the numerical study are Pr = 0.7, W/L=2, $Ra \leq 10^7$, A=2.5 and $0.1 \leq S/H \leq 0.9$ for the effect of heater location and S/H=0.4, H/L= 2, 4, 6 and 8 for the effect of heater size. The values of the parameters in the experimental study are Pr=0.7, A=2, S/H=0.5, W/L=1.666 and $Ra=7x10^4$, $1.1x10^5$ and $6.4x10^5$. The results are presented in the form of streamline, isotherm contours of the air in the cavity and temperature profiles in the heated wall. The heat transfer results are prescnted as local and average Nusselt numbers versus Rayleigh number.

Fluid flow Structure

The stream function was calculatcd to visualize the flow field within the enclosure. The strcamline contours are presented in Fig. 3 for the heat source locations S/H=0.2, 0.4, 0.6, and 0.8, A=2.5, W/L=2 and $Ra=10^5$. The streamlines werc assumed zero on the solid boundaries. The fluid is heated at the heater location, and rises due to the buoyaucy force. The warmed fluid is turned by the adiahatic ceiling of the enclosure and descends along the cooled wall, completing a recirculating flow pattern that occupies the entire enclosure. The negative sign for Ψ indicates clockwise circulation. As the heater is moved down along the heated wall a growth of the recirculating eddy occurs and a larger portion of the enclosure is affected by the buoyancy driven flow and the center of the cell moves down from y/H=0.84 at S/H=0.8 to nearly y/H=0.412 at S/H=0.2. The larger recirculating cell indicates that more of the cooled wall is thermally active. This is dlustrated by the predictions of the maximum stream function Ψ_{max} versus heater location S/H. The maximum stream function reflects the intensity of the mass flow in the primary recirculating cell. The predicted $|\Psi_{max}|$ for S/H= 0.2, 0.4, 0.6, and 0.8 were found to he 41.57, 41.87, 34.06, and 22.6 respectively. For S/H= 0.2, 0.4, and 0.6, a secondary recirculation zone was predicted in tlie upper left corner (which is not shown in Fig. 3 because of its small intensity), indicating a separatiou of the flow originating from the heater and rising along thc remainder of the adiabatic wall. This separation from the heated wall with subsequent movement toward the isothermal wall seems to be the best flow structure.

For the effect of the heater size, Fig. 4 shows the variation of the streamlines for constant heater location S/H=0.4, width ratio W/L=2 and different ratios of the

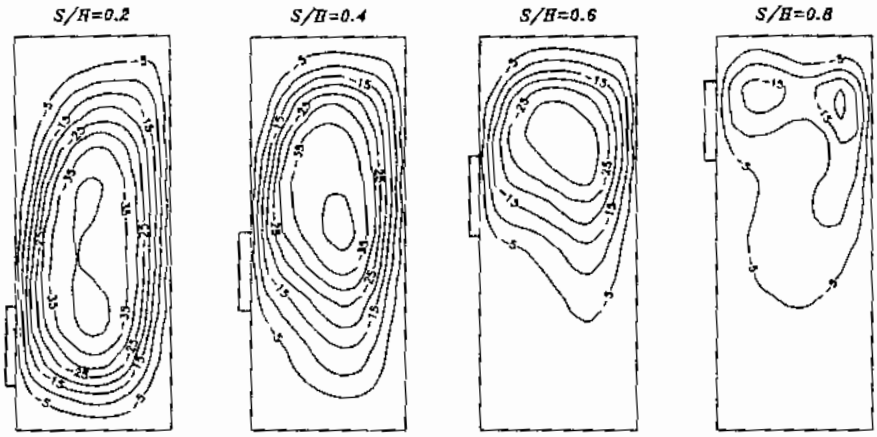

Fig. 3 Influence of heater location ratio S/H on the stream lines for A= 2.5, Pr =0.7, W/L=2, H/L=5, and Ra=10^5

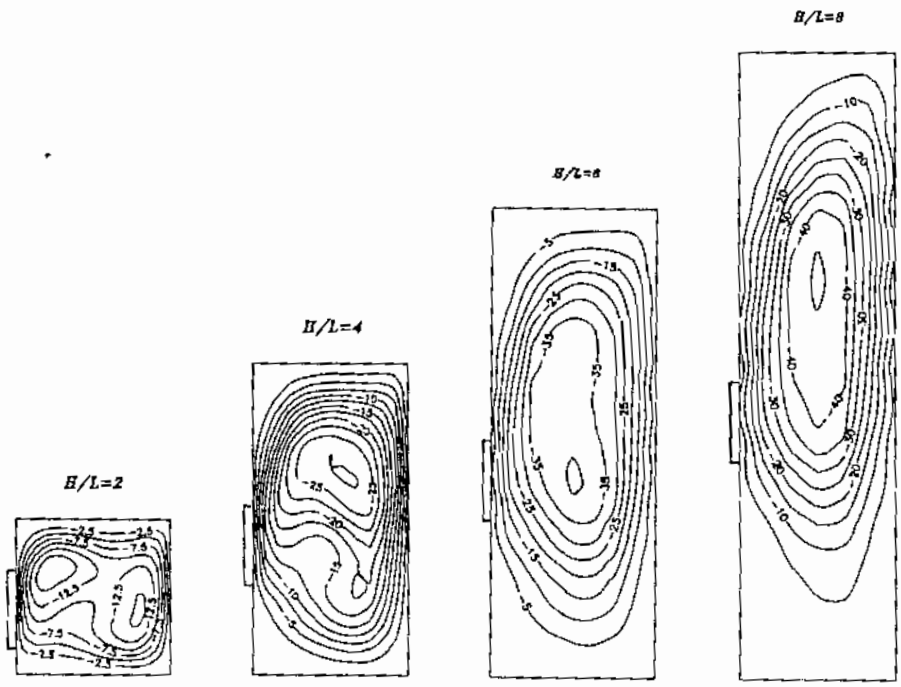

Fig. 4 Influence of heater size ratio H/L on the stream lines for A=2.5, Pr=0.7, W/L=2, S/H=0.4, and Ra=10^5

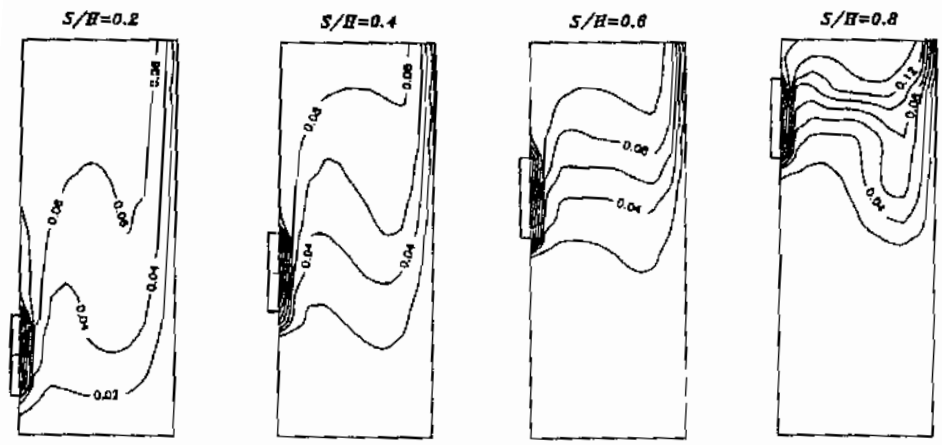

Fig. 5 Influence of heater location ratio S/H on the temperature contours for A=2.5, Pr =0.7, W/L=2, H/L=5, and Ra=10^5

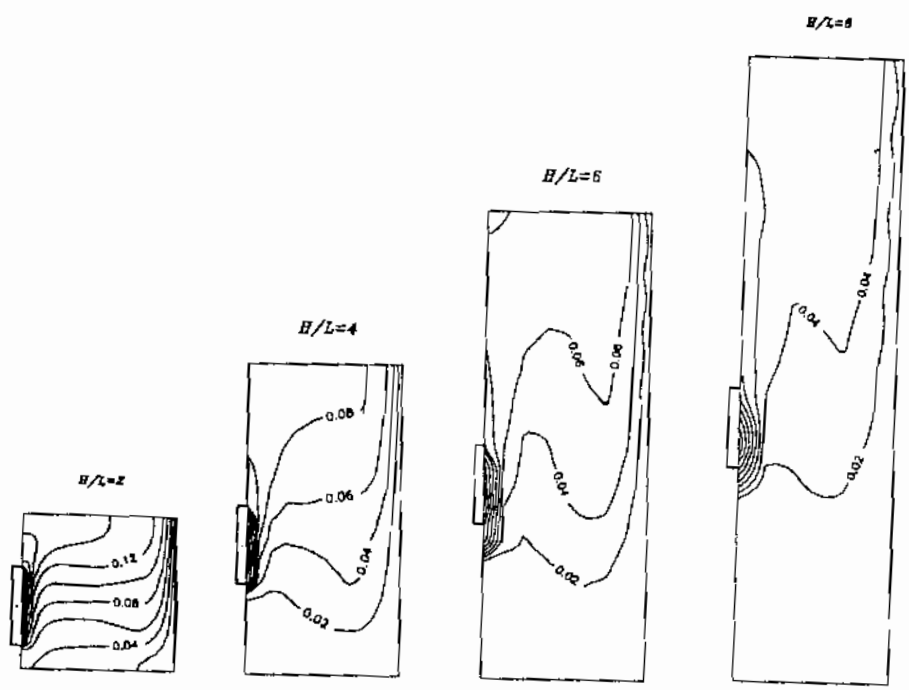

Fig. 6 Influence of heater size ratio H/L on the temperaure contours for A=2.5, Pr=0.7, W/L=2, S/H=0.4, and Ra=10^5

enclosure height to heater length H/L=2, 4, 6, and 8 for $Ra=10^5$. For the square cavity where, H/L=2, one recirculating cell including two horizontal smaller eddies occurs in the enclosure. With the increase of H/L ratio, the active height of the isothermal cold wall increases and the intensity of the mass flow increases to transfer more heat from the heater to the cold wall. Also, separation of the flow originating from the heater and rising along the remainder of the adiabatic wall increases with the increase of H/L ratio.

Isotherms

Figures 5 and 6 present dimensionless temperatures on the same format as the streamlines. In interpreting these diagrams, it should be remembered that the contour value at the isothermal cooled vertical wall equals zero. In Fig 5, the effect of heater location is presented while Fig. 6 shows the effect of heater size. The isotherms are characterized with the presence of a thermal boundary layer with dense isotherms clustered near the region of the high heat transfer along the heater for all heater locations and sizes. In Fig. 5, as the heater moves down along the wall, the more the length of the cooled isothermal wall is active, and the central region of the enclosure exhibits isothermally stable stratification. In Fig. 6, with the increase of H/L ratio and due to the increase of mass flow intensity, more heat transfers from the heater to the isothermal cooled wall and the surface heater temperature decreases.

Heater Surface Temperature

For thermal design engineers in the electronics industry, the prediction of maximum surface temperature is important. The maintenance of a proper operating temperature prolongs the life of many components and enhances their reliability. The location of the heat source in the enclosure is determined corresponding to both the maximum heater surface temperature $\theta_{h,max}$ and to the maximum heat transfer $\overline{Nu}_{max}$. The temperature results at $Ra=10^5$ for the heated and unheated sections of the wall carrying the single heater are shown in Fig. 7 for different heater locations S/H= 0.2, 0.4, 0.6 and 0.8 and in Fig. 8 for different heater size H/L=2, 4, 6 and 8. The surface temperature is characterized by gradual increase up to the surface heater, sharp rise in the surface heater temperature due to the heat input, and followed by gradual decay downstream. For all S/H values (heater locations) in Fig. 7, and all H/L values (heater sizes) in Fig. 8, the local heater surface temperature θ_h is seen to rise with increasing distance from the leading (lower) edge; i.e. the maximum heater surface temperature $\theta_{h,max}$ occurs nearly at the trailing (upper) edge. The variation of the maximum heater surface temperature $\theta_{h,max}$ with S/H ratio is shown in Fig. 9, and with H/L ratio is shown in Fig. 10 for different values of Rayleigh number. The heater location corresponding to the minimum value of $\theta_{h,max}$ differs with Ra as shown in Fig. 9. For Ra=100, the optimum heater location is nearly in the middle of the enclosure height where S/H=0.5; i.e. nearly conduction heat flow occurs. With the increase of Rayleigh number this location moves down in the lower enclosure half towards the bottom. At $Ra \geq 10^3$ the minimum values of $\theta_{h,max}$ occurs in the range of $0.1 \leq S/H \leq 0.5$ and $\theta_{h,max}$ increases with the increase of S/H for S/H >0.5; i.e. the optimum location of the heat source can be at any position in the lower half of the enclosure. In Fig. 10, for the range of H/L<4, $\theta_{h,max}$ decreases for all values of Rayleigh number with the decrease of the heater size; i.e. increase of H/L ratio, due to the relative increase of the active size of the isothermal cooled wall. For H/L≥4, $\theta_{h,max}$ is nearly constant and takes the

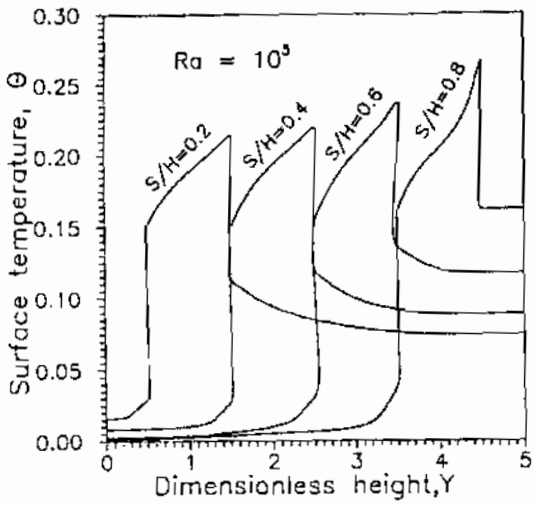

Fig. 7 Influence of heater location ratio S/H on the surface temperature for A=2.5, Pr =0.7, W/L=2, H/L=5, and Ra=10^5

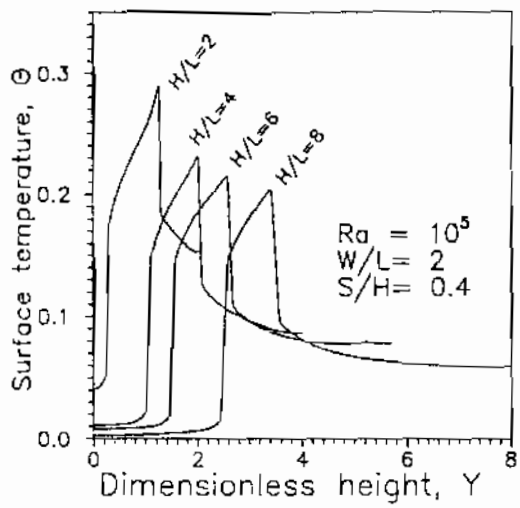

Fig. 8 Influence of the heater size ratio H/L on the surface temperature for A=2.5, Pr=0.7, W/L=2, S/H=0.4, and Ra=10^5

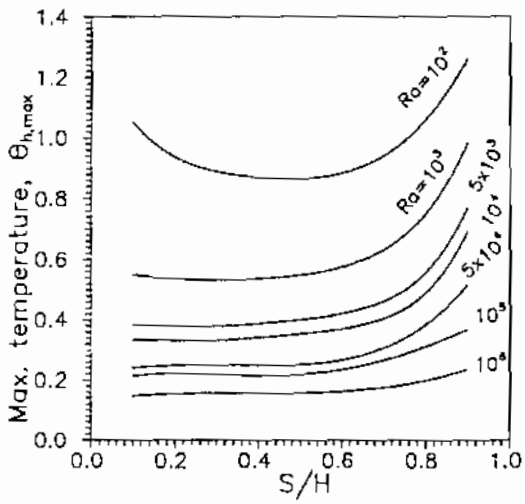

Fig. 9 Influence of heater location ratio S/H on the maximum surface temperature for A=2.5, W/L=2, and H/L=5.

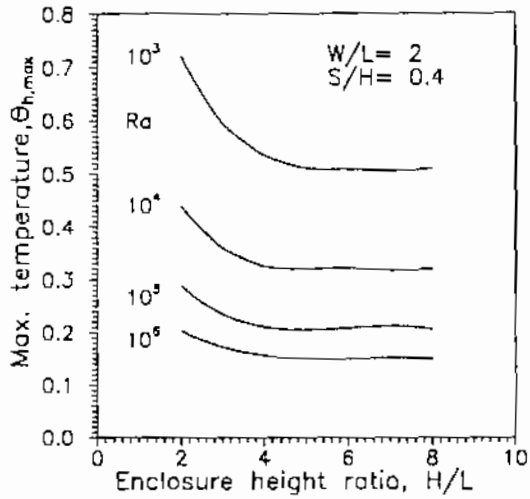

Fig. 10 Influence of the heater size ratio H/L on the maximum surfaee temperature for A=2.5, W/L=2, and S/H=0.4.

minimum values. For the optimum range of heater location and size $0.1 \le S/H \le 0.5$ and $H/L \ge 4$, the variation of $\theta_{h,max}$ with Rayleigh number is presented in Fig. 11 and correlated by

$$\theta_{max} = 1.792\ Ra^{-0.18}$$

Heat Transfer

The heat and fluid flow structures elaborated in the foregoing sections can be further inferred from the surface temperature of the constant heat flux surface heater.

The local heat transfer coefficient along the surface of the heater is presented by means of the Nusselt number according to

$$Nu = h.L/k = (q.L/k)/(T - T_w) \qquad (10)$$

which is the reciprocal of the surface local dimensionless temperature. The average heat transfer coefficient along the surface of the heater is presented by means of an average Nusselt number according to its definition for isoflux heating as:

$$\bar{Nu} = (q\,L/k)/(\bar{T}_i - T_w)] \qquad (11)$$

which is the reciprocal of the dimensionless average temperature of the surface, where $\bar{T}_i$ is the average heater surface temperature.

The distribution of the local Nusselt number along the surface heater is shown in Fig. 12 for $Ra=10^5$, $W/L=2$, and different heater locations. Fig. 13 presents the local Nu for $H/L=0.4$, $Ra=10^5$ and different heater sizes. Because the fluid approaches the leading edge of the heater source at a lower temperature, the maximum value of the local Nu occurs at the leading edge of the heater. The local Nu decreases as the distance from the leading edge increases. The heater surface local Nusselt number increases with the movement of the heater towards the bottom of the enclosure; i.e. the decrease of S/H ratio, and as the heater size decreases (with the increase of H/L ratio). This is due to the increased intensity of natural convection flow in the enclosure which is reflected from the increase of Ψ_{max}. As observed in the stream function contours and Ψ_{max} data, the increased mass movement with the increase of H/L and decrease of S/H ratios, causes more interaction with the cooled isothermal wall and also, increases the active length of the isothermal cooled wall. The fluid approaching the heater is thus at lower temperatures which results in more effective cooling of the heater.

The average heater surface Nusselt number $\bar{Nu}$ which is calculated according to Eq. 11 is shown in Figs. 14 and 15. Figure 14 presents the influence of the heater location on $\bar{Nu}$ for $W/L=2$ and different values of Rayleigh number. $\bar{Nu}$ increases with the increase of Ra. For $Ra=10^2$, where nearly conduction takes place, $\bar{Nu}_{max}$ occurs at $S/H=0.5$. With the increase of Rayleigh number this location moves down in the lower portion of the enclosure. At $Ra \ge 10^3$ the maximum values of $\bar{Nu}$ occurs in the range of $0.1 \le S/H \le 0.5$ and $\bar{Nu}$ decreases with the increase of S/H for $S/H > 0.5$; i.e. the optimum location of the heat source can be at any position in the lower half of the enclosure. Fig. 15 presents the influence of the heater size on $\bar{Nu}$ for $S/H=0.4$, $W/L=2$ and $Ra=10^3, 10^4, 10^5, 10^6$. In Fig 15, for the range of $H/L<4$, $\bar{Nu}$ increases for all values of Rayleigh number with the decrease of the heater size; i.e. increase of H/L ratio, due to the relative increase of the active size of the isothermal cooled wall. For $H/L \ge 4$, $\bar{Nu}$ is nearly constant and takes the maximum values. For the optimum range of heater location and size $0.1 \le S/H \le 0.5$ and $H/L \ge 4$, the variation of $\theta_{h,max}$ with Rayleigh number is presented in Fig. 16 and correlated by

$$\bar{Nu} = 0.74\ Ra^{0.17}$$

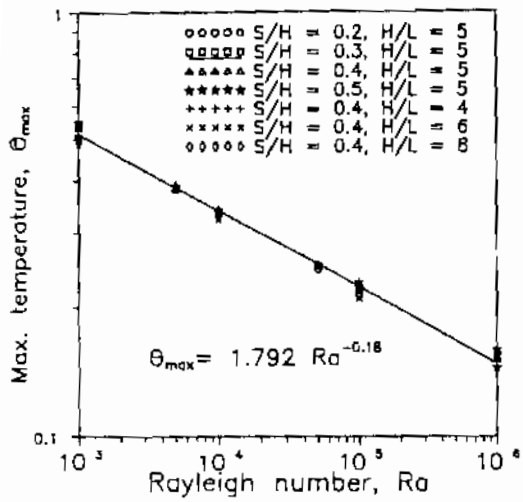

Fig. 11 Variation of heater surface maximum temperature with Rayleigh number

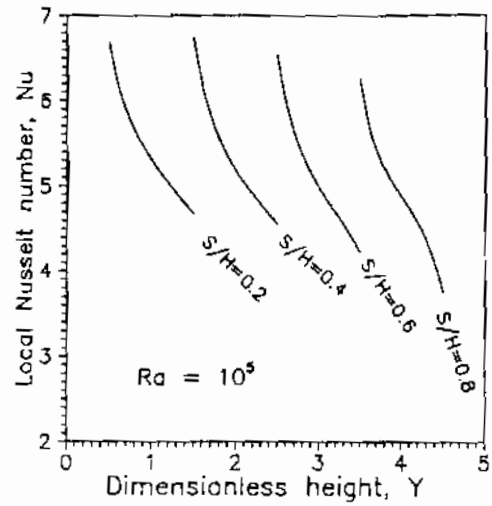

Fig. 12 Influence of heater location ratio S/H on the local Nussert number for A=2.5, W/L=2, H/L=5, and Ra=10^5

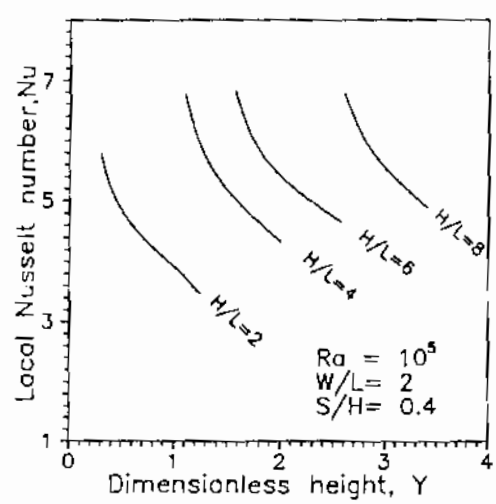

Fig. 13 Influence of the heater size ratio H/L on the local Nussert number for A=2.5, W/L=2, S/H=0.4, and Ra=10^5

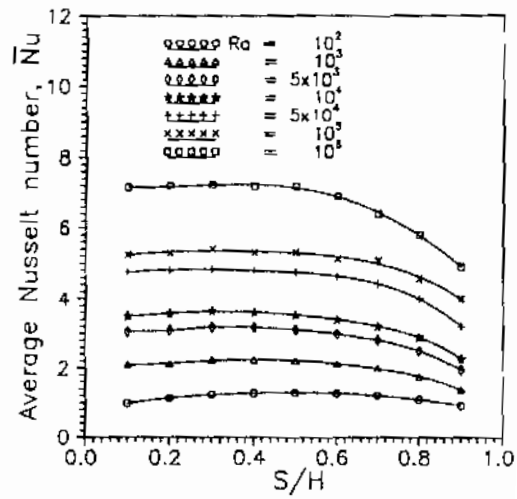

Fig. 14 Influence of heater location ratio S/H on the average Nussert number for A=2.5, W/L=2, and H/L=5.

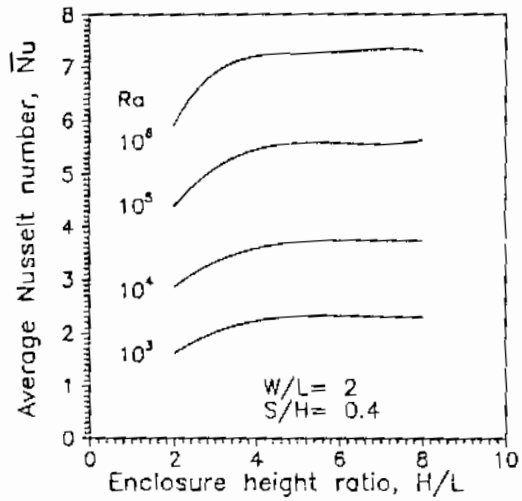

Fig. 15 Influence of the heater size ratio H/L on the average Nussert number for A=2.5, W/L=2, and S/H=0.4.

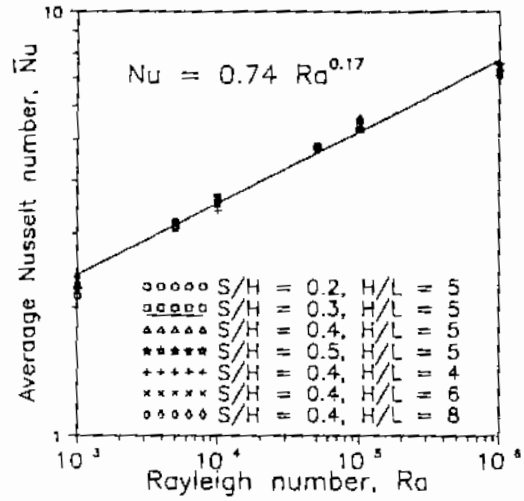

Fig. 16 Variation of heater average Nusselt number with Rayleigh number

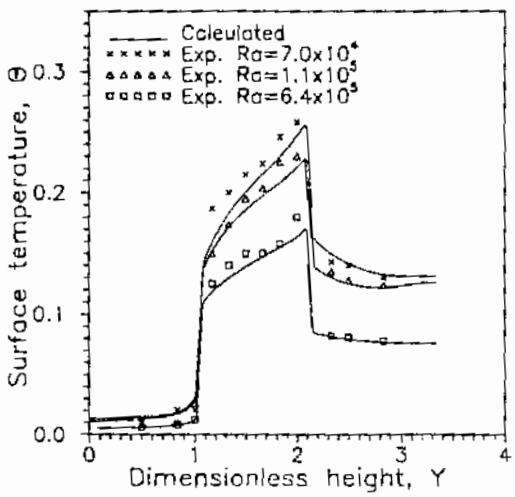

Fig. 17 Comparison between the numerical and experimental surface temperatures for A=2, W/L=1.66, H/L=3.33 and S/H=0.5

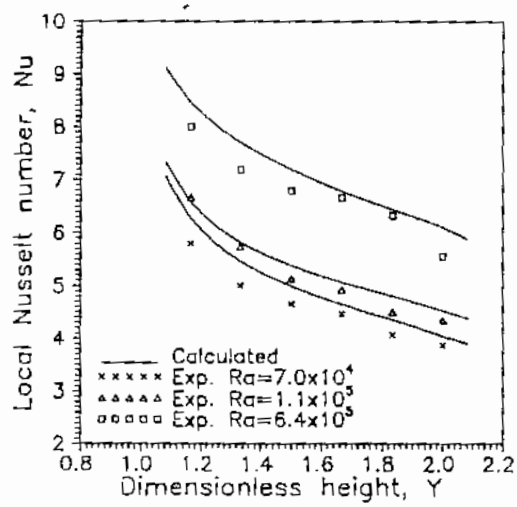

Fig. 18 Comparison between the numerical and experimental local Nusselt number for A=2, W/L=1.66, H/L=3.33 and S/H=0.5

To validate the numerically calculated results, experimental tests were done for A=2, H/L=3.33, W/L=1.66, S/H=0.5, Pr=0.7 and Ra=$7x10^4$, $1.1x10^5$ and $6.4x10^5$. Comparison is shown in Fig. 17 between the calculated local surface temperature of the heated and unheated parts of the wall and the experimental results. Fig. 18 presents a comparison between the local heater surface Nusselt number and the experimental results calculated from the experimental data according to Eq. 10. Fair agreement exists between the predicted and experimental results. The average and maximum difference between the predicted and experimental data are 7 and nearly 9 percent. respectively.

Conclusions

The effect of location and size of a single heater in a two dimensional rectangular enclosure is studied numerically. The values of the parameters considered are Pr = 0.7, W/L=2, Ra≤10^7, and A=2.5, 0.1≤S/H≤0.9 for the effect of heater location and S/H=0.4, H/L= 2, 4, 6 and 8 for the effect of heater size. The values of the parameters for the experimental study are Pr=0.7, A=2, S/H=0.5, W/L=1.66 and Ra=$7x10^4$ $1.1x10^5$, and $6.4x10^5$. The results show the following conclusions:

The local heater surface minimum temperature and the maximum value of the local Nu occurs at the leading (lower) edge; and the maximum heater surface temperature $\theta_{h,max}$ occurs at the trailing (upper) edge.

As the size of the heater decreases, or the heater moves down along the wall, a larger portion of the enclosure is affected by the buoyancy driven flow, the intensity of natural convection flow in the enclosure increases, Ψ_{max} increases causing an increase of the active length of the isothermal cooled wall, a growth of the recirculating eddy and secondary recirculation zone occurs in the upper left corner causing a separation of the flow originating from the heater, and the heater local Nusselt number increases.

With the increase of Rayleigh number, both $\bar{N}u$ and $\theta_{h,max}$ increases, the location of the heater corresponding to $\bar{N}u_{max}$ and minimum $\theta_{h,max}$ moves from the middle towards the lower portion of the enclosure. For Ra≥10^3, the optimum location and optimum size of the heater corresponding to both $\bar{N}u_{max}$ and minimum $\theta_{h,max}$ lies in the range of 0.1≤S/H≤0.5 and H/L≥4. In this range both $\bar{N}u$ and $\theta_{h,max}$ are correlated with Rayleigh number as follows:

$$\theta_{max} = 1.792\ Ra^{-0.18}\ , \qquad \bar{N}u = 0.74\ Ra^{0.17}$$

Nomenclature

A	aspect ratio, H/W
g	gravitational acceleration, m/s^2
H	enclosure height, m
k	fluid thermal conductivity, W/mK
L	heater height, m
Nu	local Nusselt number on the heater surface, Eq. (10)
$\bar{N}u$	average Nusselt number, Eq. (11)

P	pressure, Pa
Pr	fluid Prandle number, υ/α
q	heat flux on the heater surface, W/m^2
Ra	fluid Rayleigh number, $Ra = g\,\beta\,L^4\,q\,/(k\alpha\upsilon)$
S	height of heater center, m
T	temperature, K
u	air velocity in the x direction, m/s
U	non-dimensional air velocity in the X direction, u L/υ
v	air velocity in the y direction, m/s
V	non-dimensional air velocity in the Y direction, v L/υ
W	enclosure width, m
x	distance in horizontal direction, m
X	dimensionless distance in x direction, x/L
y	distance in vertical direction, m
Y	dimensionless distance in y direction, y/L
α	fluid thermal diffusivity, m^2/s
β	volumetric coefficient of thermal expansion, 1/K
θ	dimensionless temperature, $(T-T_w)/(q.L/k)$
ψ	stream function, m^2/s
Ψ	nondimensional stream function, ψ/υ
ζ	vorticity, 1/s
ω	nondimensional vortieity, $\zeta L^2/\upsilon$
υ	fluid kinematic viscosity, m^2/s
ρ	fluid density, kg/m^3

References

1. Jaluria, Y., "Natural Convective Cooling of Electronic Equipment, in Natural convection, Fundamentals & Applications" Kakac, S., Aung, V., and Viskanta, R., Hemisphere Publishing corporation, pp. 961-986, 1985.
2. Incropera, F., P., "Convection Heat Transfer in Electronic Equipment Cooling," ASME J. of Heat Transfer, Vol. 110, pp. 1097-1111, 1988.
3. Papanicolaou, E., and Jaluria, Y., "Mixed Convection From Simulated Electronic Components at Varying Relative Positions in a Cavity," ASME J. of Heat Transfer, Vol. 116, pp. 960-970, 1994.
4. Habchi, S., and Acharya, S., "Laminar Mixed Convection in a Partially Blocked, Vertical Channel," Int. J. Heat Mass Transfer, Vol. 29, pp. 1711-1722, 1986
5. Kang, B. H., Jaluria, Y., and Tewari, S. S., "Mixed Convection Transport From an Isolated Heat Source Module on a Horizontal Plate." ASME J. of Heat Transfer, Vol. 112, pp. 653-661, 1990.
6. Mahaney, H., Incropera, F., and Ramadhyani, S.,"Comparison of Predicted and Measured Mixed Convection Heat Transfer From an Array of Discrete Sources in a Horizontal Rectangular Channel," Int. J. Heat Mass Transfer, Vol. 33, No. 6, pp. 1233-1245, 1990

7. Kim, S., Sung, H., and Hyun, J., "Mixed Convection From Multiple-Layered Boards With Cross-Streamwise Periodic Boundary Conditions," Int. J. Heat Mass Transfer, Vol. 35, No. 11, pp. 2941-2952, 1992
8. Incropera, F. P., Kerby, J.S., Moffatt, D.F., and Ramadhyani, S., "Conjugate Heat Transfer from Discrete Heat Sources in a Rectangular Channel," Int. J. Heat Mass Transfer, Vol. 29, No. 7, pp. 1051-1058, 1986
9. Davalath J., and Bayazitoglu, Y, "Forced Convection Cooling Across Rectangular Blocks," ASME J. of Heat Trausfer, Vol. 109, pp. 321-328, 1987.
10. Kim, S. H., and Anand, N. K., "Turbulent Heat Transfer Between a Series of Parallel Plates With Surface-Mouuted Discrete Heat Sources," ASME J. of Heat Transfer, Vol. 116, pp. 577-587, 1994.
11. Kim, S. H., and Anand, N. K., "Laminar Developing Flow and Heat Transfer Between a Series of Parallel Plates With Surface-Mounted Discrete Heat Sources," Int. J. Heat Mass Transfer, Vol. 37, No. 15, pp. 2231-2244, 1994
12. Kim, S. H., and Anand, N. K., "Laminar Heat Transfer Between a Series of Parallel Plates With Surface-Mounted Discrete Heat Sources," ASME J. of Electronic Packaging , Vol. 117, pp. 52-62, 1995
13. Nakayama, W., and Park, S. H., "Conjugate Heat Transfer From a Single Surface-Mounted Block to Forced Convective Air Flow in a Channel," ASME J. of Heat Transfer, Vol. 118, pp. 301-308, 1996.
14. Kim, S. Y., Sung, H. J., and Hyun, J. M., "Mixed Convection From Multiple-Layered Boards With Cross-Streamwise Periodic Boundary Conditions," Int. J. Heat Mass Transfer, Vol. 35, No. 11, pp. 2941-2952, 1992
15. Jaluria, Y., "Buoyancy-Induced Flow Due to Isolated Sources on a Vertical Surface," ASME J. of Heat Transfer, Vol. 104, pp. 223-227, 1982.
16. Anand, N., Kim, S., and Aung, W., "Effect of Wall Conduction of Free Convection Between Asymmetrically Heated Vertical Plates: Uniform Wall Temperature," Int. J. Heat Mass Transfer, Vol. 33, pp. 1025-1028, 1990.
17. Kim, S., Anand, N., and Aung, W., "Effect of Wall Conduction of Free Convection Between Asymmetrically Heated Vertical Plates: Uniform Wall Heat Flux," Int. J. Heat Mass Transfer, Vol. 33, pp. 1013-1023, 1990.
18. Kim, S., Anand, N., and Fletcher, L., "Free Convection Between Series of Vertical Parallel Plates With Embedded Line Heat Sources," ASME J. of Heat Transfer, Vol. 113, pp. 108-115, 1991.
19. Keyhani, M., Prasad, M., and Cox, R., "An Experimental Study of Natural Convection in a Vertical Cavity with Discrete Heat Sources," ASME J. of Heat Transfer, Vol. 110, pp. 616-624, 1988.
20. Carnona, R., and Keyhani, M., "The Caviry Width Effect on Immersion Cooling of Discrete Flush-Heaters on One Vertical Wall of an Euclosure Cooled From the Top," ASME Journal of Electronic Packaging, Vol. 111, pp. 268-276, 1989.
21. Keyhani, M., Chen, L, and Pitts, D., "Aspect Ratio Effect on Natural Convection in an Enclosure With Protruding Heat Sources," ASME J. of Heat Transfer, Vol. 113, pp. 883-891, 1991.
22. Patankar, S., "Numerical Heat Transfer and Fluid Flow" Mc Graw Hill, New York, 1980.